

AP42 Section: 13.2.5 Industrial Wind Erosion

**Title: Background Document for AP-42 Section 11.2.7 (13.2.5 Fifth
edition) on Industrial Wind Erosion**

**MRI Report
EPA Contract 68-02-4395**

July 1988

BACKGROUND DOCUMENT FOR AP-42 SECTION 11.2.7
ON INDUSTRIAL WIND EROSION

FINAL REPORT

EPA Contract No. 68-02-4395
Assignment No. 5
MRI Project No. 8985-K(05)

July 27, 1988

For

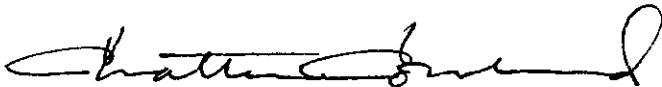
Monitoring and Data Analysis Division (MD-14)
Office of Air Quality Planning and Standards
U.S. Environmental Protection Agency
Research Triangle Park, North Carolina 27711

Attn: Mr. Dennis Shipman

PREFACE

This final report was prepared for the U.S. Environmental Protection Agency (EPA), Office of Air Quality Planning and Standards (OAQPS) under EPA Contract No. 68-02-4395, Assignment No. 5. Mr. Frank M. Noonan, Air Management Technology Branch, was the requestor of this work. Upon Mr. Noonan's retirement, Mr. Dennis Shipman became the work assignment manager. The final report was prepared by Dr. Chatten Cowherd with assistance from Dr. Gregory E. Muleski and Ms. Mary Ann Grelinger.

MIDWEST RESEARCH INSTITUTE



Chatten Cowherd, Director
Environmental Systems Department

July 27, 1988

CONTENTS

	<u>Page</u>
Preface.....	ii
1.0 Introduction.....	1
1.1 Upwind-downwind sampling.....	1
1.2 Wind tunnel sampling.....	2
1.3 Pertinent test reports.....	3
2.0 Review of Test Reports.....	5
2.1 Test Reports 1 and 2 (1984).....	5
2.2 Test Report 3 (1983).....	7
2.3 Test Report 4 (1985).....	9
2.4 Test Report 5 (1986).....	9
3.0 Emission Factor Development.....	13
3.1 Factors affecting wind erosion.....	13
3.2 Proposed emission factor.....	14
3.3 Example calculation--wind erosion emissions from conically shaped coal pile.....	23
3.4 Example calculation--wind erosion from flat area covered with coal dust.....	27
4.0 References.....	29
Appendix	
A. Estimation of Threshold Friction Velocity.....	A-1

1.0 INTRODUCTION

Wind erosion constitutes a fugitive dust entrainment mechanism distinctly different from the mechanical entrainment mechanisms associated with the other fugitive dust sources discussed in AP-42 Section 11.2. While emissions from the other sources can occur under very light breezes or even in the absence of winds, significant wind erosion emissions occur only at wind speeds above a "threshold" value. Moreover, the rate of wind erosion is strongly wind speed dependent above the threshold value. These phenomenon are widely documented in the classical studies of agricultural wind erosion.

Thus, in the estimation of wind-generated emissions, the probability that the wind speed exceeds a threshold velocity during the averaging time of interest must be addressed. Note also that, because this probability depends on the averaging time, wind erosion emission factors must include some time dependence. Emissions from other fugitive dust sources in Section 11.2, however, can be estimated using source activity measures that are not uniquely dependent on time (e.g., vehicle miles traveled, tons transferred, etc.).

1.1 UPWIND-DOWNWIND SAMPLING

The first emission factor to appear in the air pollution literature for storage pile wind erosion incorporated a simplified approach to wind speed dependence. This is largely attributable to the use of upwind-downwind sampling¹ to measure windblown suspended particulate emissions from a given quantity of stored aggregate material. This method relies on the use of an atmospheric dispersion model to back-calculate the emission rate which produces the pattern of particulate concentrations measured in the vicinity of the eroding surface. Usually the surface is represented either as a virtual point source or as a uniformly emitting area source, and wind conditions are assumed constant and unaffected by the presence of the source. The errors attributable to these simplifying assumptions are more significant for storage piles and increase with increasing pile height.

The upwind-downwind method is beset with practical difficulties for the study of wind erosion, in that the onset of erosion and its intensity are beyond the control of the investigator. As an illustration of this point, two widely cited emission factors for coal pile wind erosion were both developed from upwind-downwind sampling under light wind conditions. The factor developed by Blackwood and Wachter² was based on four tests of a coal pile with wind speeds ranging from 1.5 to 2.7 m/sec (3.4 to 6.0 mph). The emission factor developed by PEDCo Environmental³ for coal pile wind erosion and maintenance activities at western surface coal mines was based on 16 tests of three piles with wind speeds ranging from 0.2 to 3.4 m/sec (0.5 to 7.6 mph).

These upwind-downwind studies of coal pile erosion were used to derive emission factor equations accounting for the dependence of emission rate on wind speed. In both equations, erosion rate was depicted as a time independent function of wind speed over the full range of nonzero wind speed values. However, as stated above, this is inconsistent with the classical field studies of agricultural wind erosion, which have shown that the erosion rate is negligible below a threshold wind speed⁴ and is a function of wind speed above the threshold value.

The emission factor equation currently appearing in Section 11.2.3 for storage pile wind erosion was developed from upwind-downwind testing of an active storage area at a sand and gravel plant. However, a correction factor accounting for the frequency that the wind speed exceeded the threshold value (assumed to be 12 mph) was included. In other words, according to the equation, no erosion occurs at wind speeds below 12 mph, and the erosion rate is constant (independent of wind speed) for wind speeds above 12 mph.

1.2 WIND TUNNEL SAMPLING

An alternative approach to upwind downwind sampling in developing emission factors for wind erosion entails the use of a portable open-floored wind tunnel for in situ measurement of dust emitted from representative test pile surfaces under predetermined wind conditions. In effect, the experimental problem is divided into two parts: determination of the relationship between the rate of windblown dust emissions and the physical parameters which enter into the wind erosion process; and analysis of wind flow patterns around storage piles.

The wind tunnel method relies on a straightforward mass balance technique for calculation of emission rate. By sampling under light ambient wind conditions, background interferences from upwind erosion sources can be avoided. Although a portable wind tunnel does not generate the larger scales of turbulent motion found in the atmosphere, the turbulent boundary layer formed within the tunnel simulates the smaller scales of atmospheric turbulence. It is the smaller scale turbulence which penetrates the wind flow in direct contact with the pile surface and contributes to the particle entrainment mechanisms.⁵

In an early field study using a portable wind tunnel to measure suspended particulate emissions generated by wind erosion of a coal storage pile, Cowherd⁶ reported that the rate of erosion decreased sharply with time at fixed wind speeds above the threshold values. This meant that steady-state erosion could not be sustained at a fixed wind speed because of the finite availability of erodible particles on the coal pile surface, in the absence of any mechanical disturbance of the surface. This seemed to add a new level of complication to the development of emission factors for bulk aggregate materials, which typically contain a large proportion of nonerodible elements which tend to stabilize surfaces.

1.3 PERTINENT TEST REPORTS

Using the criteria specified in Section 3 of the previously submitted companion final report, five documents containing field test data on wind erosion were identified. These reports are listed in Table 1. In all cases, the wind tunnel sampling method was used to generate field data on wind erosion from open storage piles and exposed areas. Test Report 1 is a symposium paper which contained supplementary analysis of data from the primary data source (Test Report 2). Test Report 5 comprises an abbreviated presentation in the form of a symposium paper with no reference to a more comprehensive report. In the sections below, each report is discussed in terms of (a) field sampling methodology, and (b) the types and locations of test sites.

TABLE 1. PRIMARY TEST REPORTS

No.	Reference
1	Cowherd, C., Jr., "A New Approach to Estimating Wind-Generated Emissions from Coal Storage Piles," Presented at the APCA Specialty Conference on Fugitive Dust Issues in the Coal Use Cycle, Pittsburgh, PA, April 1983.
2	Axetell, K., and C. Cowherd, Jr., "Improved Emission Factors for Fugitive Dust from Surface Coal Mining Sources," Volumes I and II, U.S. EPA, Cincinnati, OH, EPA-600/7-84-048, March 1984.
3	Cuscino, T., G. E. Muleski, and C. Cowherd, Jr., "Iron and Steel Plant Open Source Fugitive Emission Control Evaluation," Final Report Prepared for the Industrial Environmental Research Laboratory, U.S. EPA, Research Triangle Park, NC (EPA Contract No. 68-02-3177, Work Assignment No. 4), August 31, 1983.
4	Muleski, G. E., "Coal Yard Wind Erosion Measurement," Final Report Prepared for Industrial Client of Midwest Research Institute, Kansas City, MO, March 1985.
5	Connor, A. D., T. E. McGuire, and M. S. Greenfield, "Erosion Testing by Portable Wind Tunnel at an Iron and Steel Plant," Presented at the 79th Annual Meeting of APCA, Minneapolis, MN, June 1986.

2.0 REVIEW OF TEST REPORTS

This section summarizes the five test reports identified in Table 1.

2.1 TEST REPORTS 1 AND 2 (1984)

In Test Report 1, Cowherd reported the results of the wind tunnel testing of coal piles at three western surface coal mines under dry conditions. Other erodible materials tested included overburden and scoria. Field testing was conducted in three coal fields: Powder River Basin (Mine 1), North Dakota (Mine 2), and Four Corners (Mine 3). A pull-through wind tunnel with a 30-cm by 3.5-m open-floored test area was used for this study. The tunnel effluent was drawn through an emissions sampling module from which particulate samples were collected isokinetically and separated into aerodynamic particle size fractions. Further detail on the design of the wind tunnel and the emissions sampling module is described in the primary data source (Test Report 2).

The loss of erodible material (g/m) which occurred during a test was calculated as follows:

$$L = \frac{CQT}{A} \quad (1)$$

where: C = time averaged particulate concentration in tunnel exit stream
(after subtraction of inlet concentration), g/m³
Q = tunnel flow rate, m³/sec
t = duration of sampling, sec
A = exposed test area = 0.918 m²

Prior to each test series, the test section of the tunnel was placed directly on the selected test surface. Care was taken not to disturb any natural crust that might be present. Location of a suitable test surface was aided by the fact that the test piles tended to be large flat areas. With the tunnel in place, the airflow was gradually increased up to the threshold for the onset of wind erosion and then reduced slightly. At the subthreshold flow, a wind speed profile was measured.

The wind speed profile near the test surface (tunnel floor) was found to follow a logarithmic distribution:

$$u(z) = \frac{u^*}{0.4} \ln \frac{z}{z_0} \quad (2)$$

where: u = wind speed, cm/sec
 u^* = friction velocity, cm/sec
 z = height above test surface, cm
 z_0 = roughness height, cm

The roughness height of each test surface was determined by extrapolation of the wind speed profile near the surface to $u(z_0)=0$. The calculated roughness height allowed for later conversion of the tunnel centerline wind speed to the equivalent wind speed at a standard 10 m height using the logarithmic wind speed profile.

On nearly all of the surfaces tested, emission rates at constant wind speeds were found to decay sharply with time due to the presence of non-erodible elements on the surface. An exception was the sandy topsoil tested at Mine 3; in that case, an increase in emission rate was observed, probably because of the entrainment effect of infiltration air as the loose soil surface receded below the sides of the wind tunnel.

Consistent with these results, it was hypothesized that the loss rate from most surfaces is proportional to the amount of erodible material remaining:

$$\frac{dM}{dt} = -kM \quad (3)$$

where: M = quantity of erodible material present on the surface at any time, g/m²
 k = constant, sec⁻¹
 t = cumulative erosion time, sec

Integration of Eq. (3) yields:

$$M = M_0 e^{-kt} \quad (4)$$

where: M_0 = erosion potential, i.e., quantity of erodible material present on the surface before the onset of erosion, g/m²

In support of this model, the cumulative erosion loss at a fixed wind speed was found to asymptotically approach a limiting value.

Consistent with Eq. (4), the erosion potential was calculated from the losses of erodible material from the test surface for two erosion times:

$$\frac{\ln\left(\frac{M_0 - L_1}{M_0}\right)}{\ln\left(\frac{M_0 - L_2}{M_0}\right)} = \frac{t_1}{t_2} \quad (5)$$

where: L_1 = loss during time period 0 to t_1 , g/m²
 L_2 = loss during time period 0 to t_2 , g/m²

An iterative procedure was required to calculate erosion potential from Eq. (5) after substitution of two cumulative loss values and erosion times obtained from back-to-back testing of the same surface.

Table 2 lists the site and sampling parameters for the wind tunnel tests at western surface coal mines. Also given are the calculated values of erosion potential classified by erodible surface type and by wind speed at the tunnel centerline. SP (suspended particulate) denotes particles equal to or smaller than 30 μ m in aerodynamic diameter, and IP (inhalable particulate) denotes particles equal to or smaller than 15 μ m in aerodynamic diameter.

2.2 TEST REPORT 3 (1983)

In Test Report 3, Cuscino et al. reported the results of wind tunnel testing at two integrated iron and steel plants in Ohio and Indiana. The following tests of uncontrolled emissions were performed using the wind tunnel method:

- Fourteen tests of wind erosion from coal storage piles
- Two tests of wind erosion from an active exposed area
- One test of wind erosion from an inactive exposed area

The design of the portable wind tunnel and the emission sampling methodology were the same as described above. However, single integrated samples of longer duration were used in place of back-to-back samples to determine erosion potential at a given wind speed.

Test plots at the two plants were formed by plant personnel. At the Ohio plant, a small level area for uncontrolled testing was formed from the steam coal storage pile with a bulldozer.

At the Indiana plant, the test plot was prepared by having a front-end loader form a layer of coal approximately 12 m by 15 m by 15 cm (40 ft by 50 ft by 6 in.) in an area of the coal yard which was not heavily traveled. The use of a front-end loader at the Indiana plant resulted in a compacted surface which was not representative of piles in the plant. For this reason, some test areas within the plot were also prepared by turning the surface with a shovel.

TABLE 2. WESTERN COAL MINE WIND EROSION SOURCE TESTING INFORMATION (TEST REPORTS 1 AND 2)

Material	Location/ description	Site	Test date	Before erosion		Roughness height, z_0 (cm)	Threshold wind speed ^a (m/s) (mph)	Erosion wind speed ^a (m/s) (mph)	Erosion potential (g/m ²)	IP/SP ^b ratio	
				Silt content (%)	Moisture content (%)						
Pulverized coal	Area surrounding recently active pile	Western surface coal mine 1	11/9/79	16.4	2.5	0.01	10	12	> 15 ^c	0.62	
			11/9/79	16.4	2.5	10	21	14	32		52 ^c
Coal	Uncrusted pile	Western surface coal mine 2	11/4/79	11.6	2.8	0.3	11	13	26	8 ^c	0.68
			11/3/79	5.1	20.2	14	32	14	26	3.4	
			11/3/79	5.1	20.2	14	32	17	29	16	
			11/4/79	3.4	6.8	14	32	17	32	15	
Coal	Lightly crusted tracks on pile	Western surface coal mine 3	8/12/80	3.8	4.6	0.06	9	12	26	8 ^c	0.55
			8/13/80	4.4	3.4	8	19	12	26	3.4	
			8/12/80	3.8	4.6	9	20	13	29	16	
			8/13/80	3.8	4.6	9	20	14	32	29	
Coal	Pile furrow	Western surface coal mine 3	8/12/80-8/13/80	4.0	7.8	0.05	15	16	35	7.5	0.60
			8/13/80-8/13/80	4.0	7.8	15	33	17	38	10	
Overburden	-	Western surface coal mine 2	11/2/79	21.1	6.4	0.3	10	16	35	10	0.68
			11/2/79	21.1	6.4	10	23	17	38	5 ^c	
Scoria	Roadbed material	Western surface coal mine 2	11/5/79	18.8	4.1	0.3	13	16	35	11	0.75

a At tunnel centerline, 15 cm above surface.

b Calculated for each location in Test Report 1.

c Estimated value.

d Erosion loss may have occurred prior to testing.

Table 3 lists the site and sampling parameters for the wind tunnel tests at the midwestern steel plants. Also given are the calculated values of erosion potential classified by erodible surface type and by wind speed at the tunnel centerline. TP denotes total airborne particulate matter; IP (inhalable particulate matter) denotes particles equal to or smaller than 15 μm in aerodynamic diameter; and FP (fine particulate matter) denotes particles equal to or smaller than 2.5 μm aerodynamic diameter.

2.3 TEST REPORT 4 (1985)

In Test Report 4, Muleski reported the results of wind tunnel testing at an eastern power plant. Nine tests of wind generated emissions from coal surfaces were performed. The design of the portable wind tunnel and the emission sampling methodology were the same as described above (Section 2.1). However, single integrated samples of longer duration were used in place of back-to-back samples to determine erosion potential at a given wind speed.

Table 4 lists the site and sampling parameters for the wind tunnel tests at the power plant. Also given are the calculated values of erosion potential classified by erodible surface type and by wind speed at the tunnel centerline. TP denotes total particulate matter; SP denotes suspended particulate matter consisting of particles equal to or smaller than 30 μm in aerodynamic diameter; IP denotes inhalable particulate matter consisting of particles equal to or smaller than 15 μm in aerodynamic diameter; PM_{10} denotes thoracic particulate matter consisting of particles equal to or smaller than 10 μm in aerodynamic diameter; and FP denotes fine particulate matter consisting of particles equal to or smaller than 2.5 μm in aerodynamic diameter.

2.4 TEST REPORT 5 (1986)

In Test Report 5, Connor et al. reported the results of wind tunnel testing at a Canadian steel plant. The following tests of uncontrolled emissions were performed using the wind tunnel method:

- Twelve tests of coal storage piles
- Six tests of various exposed ground areas within the plant

The design of the portable wind tunnel and the emission sampling methodology were very similar to that described above (Section 2.1). Single integrated samples of longer duration were used in place of back-to-back samples to determine erosion potential at a given wind speed. However, only total particulate emissions were determined, without any particle size classification.

Table 5 lists the site and sampling parameters for the wind tunnel tests at the Canadian steel plant. Also given are the calculated values of erosion potential classified by erodible surface type and by wind speed at the tunnel centerline.

TABLE 3. MIDWESTERN STEEL PLANT WIND EROSION SOURCE TESTING INFORMATION (TEST REPORT 3)

Material	Location/ description	Site	Test date	Before erosion		Roughness height, z_0 (cm)	Threshold wind speed ^a (m/s) (mph)	Erosion wind speed ^a (m/s) (mph)	Erosion potential (g/m ²)
				Silt content (%)	Moisture content (%)				
Steam coal	Active pile	Iron and steel plant	10/22/80	4.2	2.7	0.25	8 18	15 34	31 > 2.1 (IP) 0.91 (FP)
Steam coal	Undisturbed pile, Coherex® controlled	Iron and steel plant	10/23/80	3.0	3.6	0.004	12 27	15 34	3.2 (TP) 0.79 (IP) 0.34 (FP)
Cambria coking (10-vol) coal	Turned	Iron and steel plant	10/15/81	6.5	-	0.087	9 21	11 25	7.5 (TP) 0.30 (IP) 0.14 (FP)

^a At tunnel centerline, 15 cm above surface.

TABLE 4. EASTERN POWER PLANT WIND EROSION SOURCE TESTING INFORMATION (TEST REPORT 4)

Material	Location/ description	Site	Test date	Before erosion:		Roughness height, z_0 (cm)	Threshold wind speed ^a (m/s) (mph)	Erosion wind speed ^a (m/s) (mph)	Erosion potential (g/m ²)		
				Silt content (%)	Moisture content (%)						
Fine coal dust	On concrete pad	Eastern power plant	9/22/84	8.5	3.0	0.2	6	6	14	5.8 (TP) 1.8 (SP) 1.1 (IP) 1.1 (IP) 0.87 (PM ₁₀) 0.29 (FP)	
							8	18	32	32 (TP) 8.2 (SP) 5.9 (IP) 4.6 (PM ₁₀) 1.6 (FP)	
							10	22	78	78 (TP) 16 (SP) 11 (IP) 8.7 (PM ₁₀) 3.0 (FP)	
Coal	Day pile	Eastern power plant	9/24/84	2.4	3.4	0.003	8	18	11	24	3.8 (TP) 0.72 (SP) 0.57 (IP) 0.50 (PM ₁₀) 0.33 (FP)
							13	30	32	32 (TP) 5.3 (SP) 3.7 (IP) 2.8 (PM ₁₀) 1.1 (FP)	
							16	35	56	56 (TP) 9.2 (SP) 6.5 (IP) 5.0 (PM ₁₀) 1.9 (FP)	
Coal	Main pile between scraper tracks	Eastern power plant	9/26/84	1.8	1.9	0.07	8	18	10	23	2.0 (TP) 1.1 (SP) 0.96 (IP) 0.84 (PM ₁₀) 0.52 (FP)
							12	26	34	34 (TP) 2.0 (SP) 1.7 (IP) 1.5 (PM ₁₀) 0.94 (FP)	
							13	30	40	40 (TP) 2.3 (SP) 2.0 (IP) 1.8 (PM ₁₀) 1.1 (FP)	

^a At tunnel centerline, 15 cm above surface.

TABLE 5. CANADIAN STEEL PLANT WIND EROSION TESTING INFORMATION (TEST REPORT 5)

Material	Location/ description	Site	Test date	Before erosion		Roughness height, z ₀ (cm)	Threshold wind speed ^a (m/s) (mph)	Erosion wind speed ^a (m/s) (mph)	Erosion potential (g/m ²)	
				Silt content (%)	Moisture content (%)					
Coal	Active, smooth pile	Iron and steel plant	NA	7.1	1.9	NA	NA	9.0	20.1 (TP)	76.4 (TP)
				13.4	30.0			13.4	30.0	350 (TP)
				15.9	35.6			15.9	35.6	890 (TP)
Coal	Active, rough pile	Iron and steel plant	NA	4.5	8.9	NA	NA	8.8	19.7 (TP)	0.17 (TP)
				12.4	27.7			12.4	27.7	7.8 (TP)
				15.5	34.7			15.5	34.7	24.4 (TP)
				8.6	19.2			8.6	19.2	155 (TP)
				13.0	29.1			13.0	29.1	671 (TP)
Open area dust	Blast furnace parking lot East No. 1 hot mill North dock Ingot yard Waste transfer station Mould yard	Iron and steel plant	NA	6.9	7.0	NA	NA	15.3	34.2 (TP)	1,470 (TP)
				4.4	0.7			9.5	21.3	15.5 (TP)
				6.0	0.3			12.6	28.2	88.5 (TP)
				9.6	0.0			15.8	35.3	226 (TP)
				4.4	0.7			8.6	19.2	5.1 (TP)
				NA	NA			8.2	18.3	11.6 (TP)
				NA	NA			7.7	17.2	19.4 (TP)
Coal	Active, rough pile	Iron and steel plant	NA	13.0	0.6	NA	NA	7.7	17.2 (TP)	62.2 (TP)
				15.6	0.5			8.5	19.0	85.3 (TP)
				21.3	0.0			8.2	18.3	203 (TP)

^a At tunnel centerline, 15 cm above surface.

NA = Not available.

3.0 EMISSION FACTOR DEVELOPMENT

This section presents the rationale for recommendation of an emission factor equation for estimation of dust emissions generated by wind erosion of open aggregate storage piles and exposed areas within an industrial facility. The recommended emission factor is a refinement of that originally proposed in Test Report 1.

3.1 FACTORS AFFECTING WIND EROSION

Industrial wind erosion sources typically are characterized by nonhomogeneous surfaces impregnated with nonerodible elements (particles larger than approximately 1 cm in diameter). Field testing of coal piles and other exposed materials using a portable wind tunnel has shown that (a) threshold wind speeds exceed 5 m/s (11 mph) at 15 cm above the surface or 10 m/s (22 mph) at 7 m above the surface, and (b) particulate emission rates tend to decay rapidly (half life of a few minutes) during an erosion event. In other words, these aggregate material surfaces are characterized by finite availability of erodible material (mass/area) referred to as the erosion potential. Any natural crusting of the surface binds the erodible material, thereby reducing the erosion potential.

If typical values for threshold wind speed at 15 cm are corrected to typical wind sensor height (7-10 m), the resulting values exceed the upper extremes of hourly mean wind speeds observed in most areas of the country. In other words, mean atmospheric wind speeds are not sufficient to sustain wind erosion from flat surfaces of the type tested. However, wind gusts may quickly deplete a substantial portion of the erosion potential. Because erosion potential has been found to increase rapidly with increasing wind speed, estimated emissions should be related to the gusts of highest magnitude.

The routinely measured meteorological variable which best reflects the magnitude of wind gusts is the fastest mile. This quantity represents the wind speed corresponding to the whole mile of wind movement which has passed by the 1-mile contact anemometer in the least amount of time. Daily measurements of the fastest mile are presented in the monthly Local Climatological Data (LCD) summaries. The duration of the fastest mile, typically about 2 min (for a fastest mile of 30 mph), matches well with the half life of the erosion process, which ranges between 1 and 4 min. It should be noted, however, that peak winds can significantly exceed the daily fastest mile.⁷

The wind speed profile in the surface boundary layer is found to follow a logarithmic distribution:

$$u(z) = \frac{u^*}{0.4} \ln \frac{z}{z_0} \quad (z > z_0) \quad (6)$$

where u = wind speed, cm/sec
 u^* = friction velocity, cm/sec
 z = height above test surface, cm
 z_0 = roughness height, cm
 0.4 = von Karman's constant, dimensionless

The friction velocity (u^*) is a measure of wind shear stress on the erodible surface, as determined from the slope of the logarithmic velocity profile. The roughness height (z_0) is a measure of the roughness of the exposed surface as determined from the y-intercept of the velocity profile, i.e., the height at which the wind speed is zero. These parameters are illustrated in Figure 1 for a roughness height of 0.1 cm.

Emissions generated by wind erosion are also dependent on the frequency of disturbance of the erodible surface because each time that a surface is disturbed, its erosion potential is restored. A disturbance is defined as an action which results in the exposure of fresh surface material. On a storage pile, this would occur whenever aggregate material is either added to or removed from the old surface. A disturbance of an exposed area may also result from the turning of surface material to a depth exceeding the size of the largest pieces of material present.

3.2 PROPOSED EMISSION FACTOR

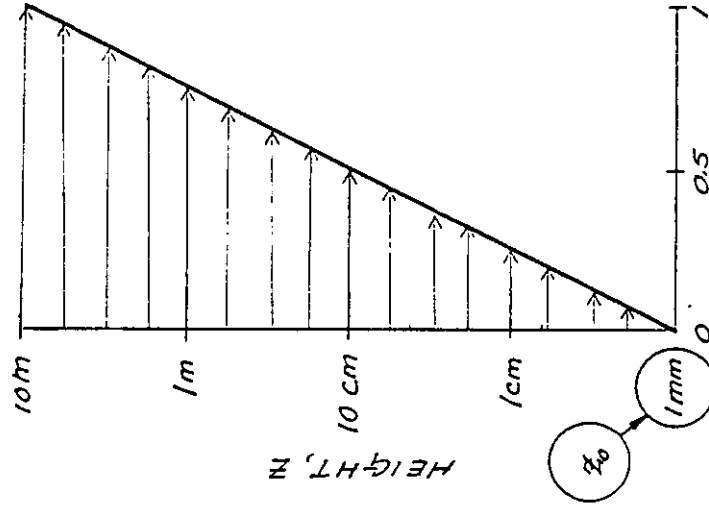
The emission factor for wind-generated particulate emissions from mixtures of erodible and nonerodible surface material subject to disturbance may be expressed in units of g/m²-yr as follows:

$$\text{Emission factor} = k \sum_{i=1}^N P_i \quad (7)$$

where k = particle size multiplier
 N = number of disturbances per year
 P_i = erosion potential corresponding to the observed (or probable) fastest mile of wind for the i th period between disturbances, g/m²

The particle size multiplier (k) for Equation 7 varies with aerodynamic particle size, as follows:

SEMI-LOGARITHMIC REPRESENTATION



ARITHMETIC REPRESENTATION

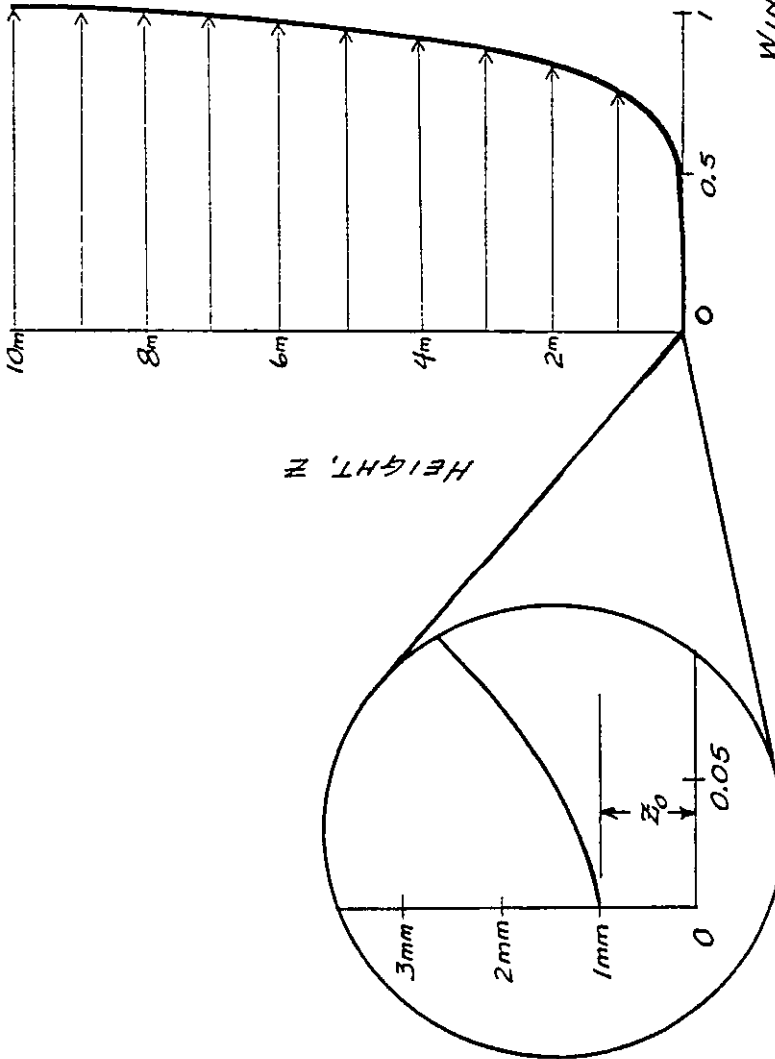


Figure 1. Illustration of logarithmic velocity profile.

AERODYNAMIC PARTICLE SIZE MULTIPLIERS FOR EQUATION 7

$< 30 \mu\text{m}$	$< 15 \mu\text{m}$	$< 10 \mu\text{m}$	$< 2.5 \mu\text{m}$
1.0	0.6	0.5	0.2

This distribution of particle size within the $< 30 \mu\text{m}$ fraction is comparable to the distributions reported for other fugitive dust sources where wind speed is a factor. This is illustrated, for example, in the distributions for batch and continuous drop operations encompassing a number of test aggregate materials (see AP-42 Section 11.2.3).

In calculating emission factors, each area of an erodible surface that is subject to a different frequency of disturbance should be treated separately. For a surface disturbed daily, $N = 365/\text{yr}$, and for a surface disturbance once every 6 months, $N = 2/\text{yr}$.

A generalized mathematical relationship for the erosion potential (P) of a typical aggregate material, as a function of the friction velocity above the threshold value ($u^* - u_t^*$) can in principle be derived from the data presented in Test Reports 1 through 4.

The most reliable values for P come from the western Mine 3 test results in Test Reports 1 and 2 and from the eastern power plant test results in Test Report 4. These data, as shown in Table 6, formed the basis for the erosion potential function. The SP size fraction represented by these data reflects potential air quality impact as measured by the standard high-volume sampler. The 50% cutpoint for this sampler can range between 25 and 50 μm in aerodynamic diameter (μmA) depending on wind speed and direction. An effective cutpoint of 30 μmA is usually assigned to the standard high-volume sampler.

The Mine 1 and Mine 2 test results contained in Test Reports 1 and 2 are judged to be less reliable because at those two sites the appearance of visible emissions was used as the indicator of the wind erosion threshold. In all other cases covered by the five test reports, the direct observation of particle movement on the surface (which occurs at a wind speed below that required to produce visible emissions) was the indicator of the erosion threshold. Also the surfaces encountered at Mine 2 were wetter than usual because of unfavorable weather conditions. Therefore the results from Mines 1 and 2 are excluded from the data base, except for the tests of scoria and the uncrusted coal pile under dry conditions.

The test results from Test Report 3 are not included because the special test plots used in that study may not be representative of realistic coal pile surfaces. The test plots in that study were formed as control surfaces for the study of the effectiveness of dust suppressants.

TABLE 6. DATA BASE FOR PREDICTIVE EQUATION

Material	u* (m/s)	u*-u* _t (m/s)	P (g/m ²) ^a	
			Obs.	Pred. ^b
Scoria (roadbed material at Mine 2)	1.33	0	0	0
	1.64	0.31	11	13.3
Fine coal dust (on concrete pad at eastern power plant)	0.54	0	0	0
	0.58	0.04	1.8	1.1
	0.74	0.20	8.2	7.3
	0.93	0.39	16	18.6
Uncrusted coal pile (Mine 2)	1.12	0	0	0
	1.33	0.21	26	7.8
	1.74	0.62	41	38.0
Lightly crusted tracks on coal pile (Mine 3)	0.58-0.65	0	0	0
	0.87	0.22	8.0	8.3
	0.87	0.29	3.4	12.1
	0.94	0.29	16	12.1
	1.01	0.36	29	16.6
	1.01	0.43	15	21.5
Coal day pile (freshly stacked at eastern power plant)	0.38	0	0	0
	0.52	0.14	0.72	4.6
	0.61	0.23	5.3	8.8
	0.75	0.37	9.2	17.2

^a SP (suspended particulate).

^b $P = 58.59 (u^* - u_t^*)^2 + 24.90 (u^* - u_t^*)$.

The test results from Test Report 5 are not included in the figures because only total particulate (TP) data are given. It is likely that very large particles transported by saltation rather than suspension were collected in the TP samples. Because saltating particles do not reach heights above about 30 cm, such particles should not be included in particulate emission factors.

Based on regression analysis of the data base in Table 6, the erosion potential function for a dry, exposed surface was found to fit the following quadratic relationship:

$$P = 58 (u^* - u_t^*)^2 + 25 (u^* - u_t^*) \quad (8)$$
$$P = 0 \text{ for } u^* \leq u_t^*$$

where u^* = friction velocity (m/s)
 u_t^* = threshold friction velocity (m/s)

This equation has a 2σ precision factor of 5.3, which represents the 95% confidence level for a log-normally distributed data set.

Equations 7 and 8 apply only to dry, exposed materials with limited erosion potential. The resulting calculation is valid only for a time period as long or longer than the period between disturbances. Calculated emissions represent intermittent events and should not be input directly into dispersion models that assume steady state emission rates. Because of the nonlinear form of the erosion potential function, each erosion event must be treated separately.

For uncrusted surfaces, the threshold friction velocity is best estimated from the dry aggregate structure of the soil. A simple hand sieving test of surface soil (adapted from a laboratory procedure published by W. S. Chepil⁸) can be used to determine the mode of the surface aggregate size distribution by inspection of relative sieve catch amounts, following the procedure specified in Appendix A. The threshold friction velocity for erosion can be determined from the mode of the aggregate size distribution, as described by Gillette.⁹ This conversion is also described in Appendix A. Threshold friction velocities for the surface types represented in the erosion potential data base are presented in Table 7.

The fastest mile of wind for the periods between disturbances may be obtained from the monthly LCD summaries for the nearest reporting weather station that is representative of the site in question.¹⁰ These summaries report actual fastest mile values for each day of a given month. Because the erosion potential is a highly nonlinear function of the fastest mile, mean values of the fastest mile are inappropriate. The anemometer heights of reporting weather stations are found in Reference 11, and should be corrected to a 10-m reference height using Equation 6.

TABLE 7. THRESHOLD FRICTION VELOCITIES

Material	Threshold friction velocity (m/s)	Roughness height (cm)	Threshold wind velocity at 10 m (m/s)		Ref.
			$z_0 = \text{Actual}$	$z_0 = 0.5 \text{ cm}$	
Overburden ^a	1.02	0.3	21	19	2
Scoria (roadbed material) ^a	1.33	0.3	27	25	2
Ground coal ^a (surrounding coal pile)	0.55	0.01	16	10	2
Uncrusted coal pile ^a	1.12	0.3	23	21	2
Scraper tracks on coal pile ^{a,b}	0.62	0.06	15	12	2
Fine coal dust on concrete pad ^c	0.54	0.2	11	10	3

^a Western surface coal mine.

^b Lightly crusted.

^c Eastern power plant.

To convert the fastest mile of wind (u^+) from a reference anemometer height of 10 m to the equivalent friction velocity (u^*), the logarithmic wind speed profile may be used to yield the following equation:

$$u^* = 0.053 u_{10}^+ \quad (9)$$

where u^* = friction velocity (m/s)

u_{10}^+ = fastest mile of reference anemometer for period between disturbances (m/s)

This assumes a typical roughness height of 0.5 cm for open terrain. Equation 9 is restricted to large relatively flat piles or exposed areas with little penetration into the surface wind layer.

If the pile significantly penetrates the surface wind layer (i.e., with a height-to-base ratio exceeding 0.2), it is necessary to divide the pile area into subareas representing different degrees of exposure to wind. The results of physical modeling show that the frontal face of an elevated pile is exposed to wind speeds of the same order as the approach wind speed at the top of the pile.

For two representative pile shapes (conical and oval with flat-top, 37 degree side slope), the ratios of surface wind speed (u_s) to approach wind speed (u_r) have been derived from wind tunnel studies.¹² The results are shown in Figure 2 corresponding to an actual pile height of 11 m, a reference (upwind) anemometer height of 10 m, and a pile surface roughness height (z_0) of 0.5 cm. The measured surface winds correspond to a height of 25 cm above the surface. The area fraction within each contour pair is specified in Table 8.

The profiles of u_s/u_r in Figure 2 can be used to estimate the surface friction velocity distribution around similarly shaped piles, using the following procedure:

1. Correct the fastest mile value (u^+) for the period of interest from the anemometer height (z) to a reference height of 10 m (u_{10}^+) using a variation of Equation 1, as follows:

$$u_{10}^+ = u^+ \frac{\ln(10/0.005)}{\ln(z/0.005)} \quad (10)$$

where a typical roughness height of 0.5 cm (0.005 m) has been assumed. If a site specific roughness height is available, it should be used.

2. Use the appropriate part of Figure 2 based on the pile shape and orientation to the fastest mile of wind, to obtain the corresponding surface wind speed distribution (u_s^+), i.e.,

$$u_s^+ = \frac{u_s}{u_r} u_{10}^+ \quad (11)$$

3. For any subarea of the pile surface having a narrow range of surface wind speed, use a variation of Equation 1 to calculate the equivalent friction velocity (u^*), as follows:

$$u^* = \frac{0.4 u_s^+}{\ln \frac{25}{0.5}} = 0.10 u_s^+ \quad (12)$$

From this point on, the procedure is identical to that used for a flat pile, as described above.

Implementation of the above procedure is carried out in the following steps:

1. Determine threshold friction velocity for erodible material of interest (see Table 6 or determine from mode of aggregate size distribution).

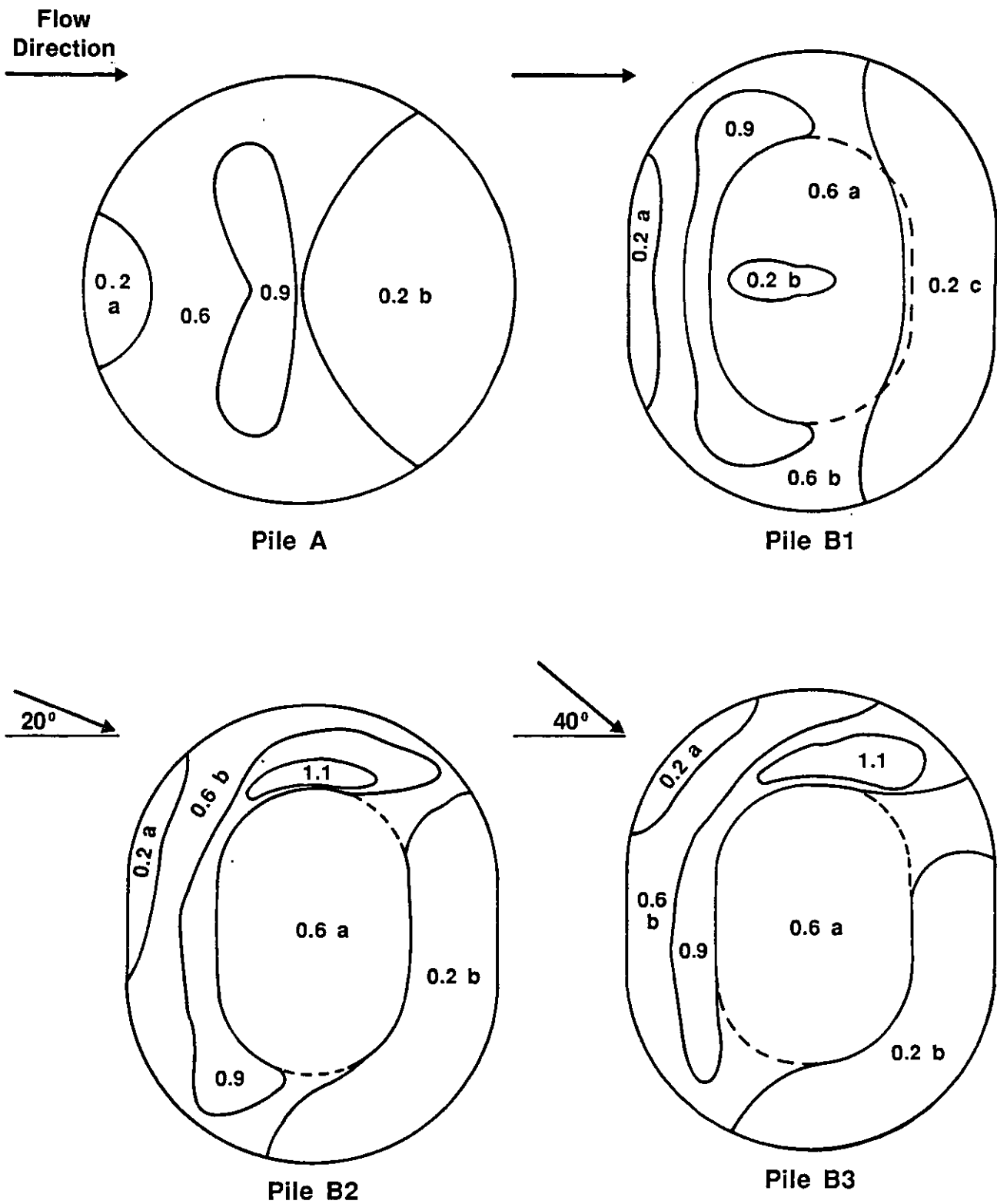


Figure 2. Contours of Normalized Surface Wind Speeds, u_s/u_r

TABLE 8. SUBAREA DISTRIBUTION FOR REGIMES OF u_s/u_r

Pile subarea	Percent of pile surface area (Figure 2)			
	Pile A	Pile B1	Pile B2	Pile B3
0.2a	5	5	3	3
0.2b	35	2	28	25
0.2c	-	29	-	-
0.6a	48	26	29	28
0.6b	-	24	22	26
0.9	12	14	15	14
1.1	-	-	3	4

2. Divide the exposed surface area into subareas of constant frequency of disturbance (N).
3. Tabulate fastest mile values (u^+) for each frequency of disturbance and correct them to 10 m (u_{10}^+) using Equation 10.
4. Convert fastest mile values (u_{10}^+) to equivalent friction velocities (u^*), taking into account (a) the uniform wind exposure of nonelevated surfaces, using Equation 9, or (b) the nonuniform wind exposure of elevated surfaces (piles), using Equations 11 and 12.
5. For elevated surfaces (piles), subdivide areas of constant N into subareas of constant u^* (i.e., within the isopleth values of u_s/u_r in Figure 2 and Table 8 and determine the size of each subarea.
6. Treating each subarea (of constant N and u^*) as a separate source, calculate the erosion potential (P_i) for each period between disturbances using Equation 8 and the emission factor using Equation 7.
7. Multiply the resulting emission factor for each subarea by the size of the subarea, and add the emission contributions of all subareas. Note that the highest 24-hr emissions would be expected to occur on the windiest day of the year. Maximum emissions are calculated assuming a single event with the highest fastest mile value for the annual period.

The recommended emission factor equation presented above assumes that all of the erosion potential corresponding to the fastest mile of wind is lost during the period between disturbances. Because the fastest mile event typically lasts only about 2 min, which corresponds roughly to the half-life for the decay of actual erosion potential, it could be argued that the emission factor overestimates particulate emissions. However, there are other aspects of the wind erosion process which offset this apparent conservatism:

1. The fastest mile event contains peak winds which substantially exceed the mean value for the event.
2. Whenever the fastest mile event occurs, there are usually a number of periods of slightly lower mean wind speed which contain peak gusts of the same order as the fastest mile wind speed.

Of greater concern is the likelihood of overprediction of wind erosion emissions in the case of surfaces disturbed infrequently in comparison to the rate of crust formation.

3.3 EXAMPLE CALCULATION--WIND EROSION EMISSIONS FROM CONICALLY SHAPED COAL PILE

A coal-burning facility maintains a conically shaped surge pile 11 m in height and 29.2 m in base diameter, containing about 2000 Mg of coal, with a bulk density of 800 kg/m³ (50 lb/ft³). The total exposed surface area of the pile is calculated as follows:

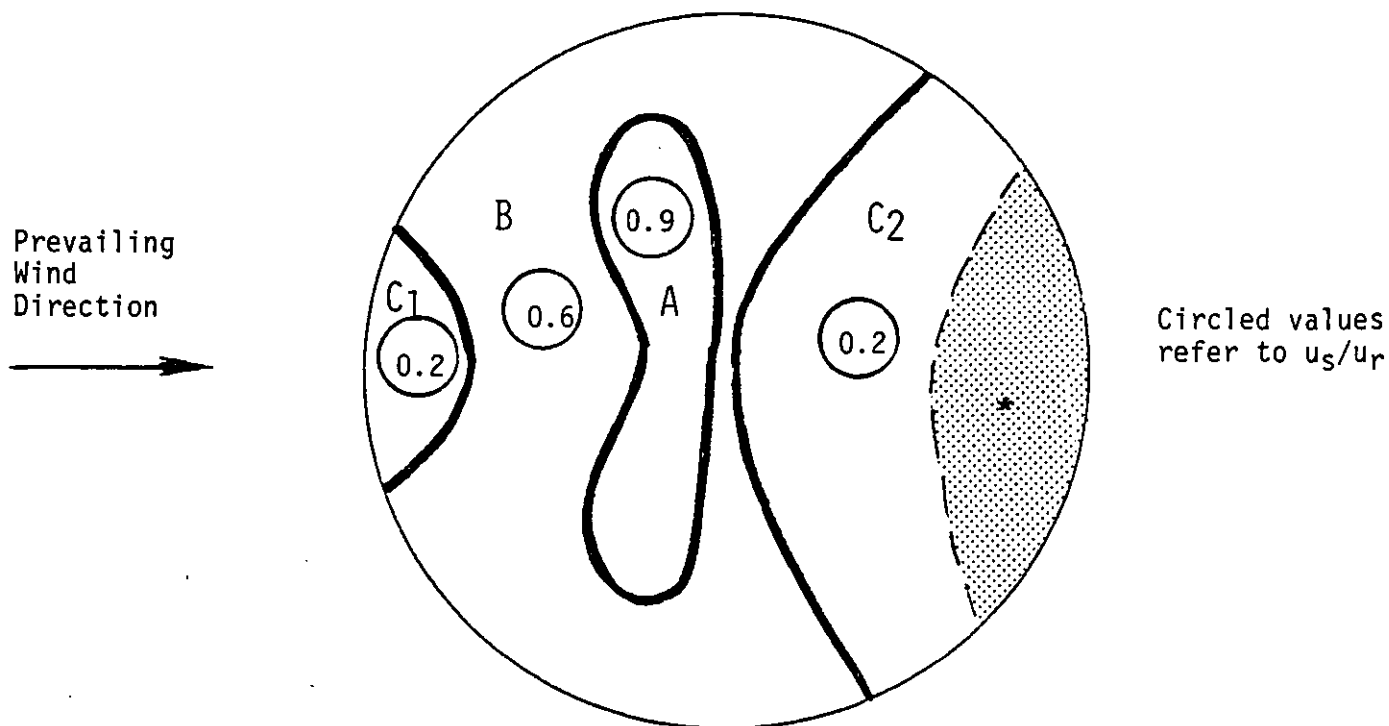
$$\begin{aligned}
 S &= \pi r \sqrt{r^2 + h^2} \\
 &= 3.14(14.6) \sqrt{(14.6)^2 + (11.0)^2} \\
 &= 838 \text{ m}^2
 \end{aligned}$$

Coal is added to the pile by means of a fixed stacker and reclaimed by front-end loaders operating at the base of the pile on the downwind side. In addition, every 3 days 250 Mg (12.5% of the stored capacity of coal) is added back to the pile by a topping off operation, thereby restoring the full capacity of the pile. It is assumed that (a) the reclaiming operation disturbs only a limited portion of the surface area where the daily activity is occurring, such that the remainder of the pile surface remains intact, and (b) the topping off operation creates a fresh surface on the entire pile while restoring its original shape in the area depleted by daily reclaiming activity.

Because of the high frequency of disturbance of the pile, a large number of calculations must be made to determine each contribution to the total annual wind erosion emissions. This illustration will use a single month as an example.

Step 1: In the absence of field data for estimating the threshold friction velocity, a value of 1.12 m/s is obtained from Table 6.

Step 2: Except for a small area near the base of the pile (see Figure 3), the entire pile surface is disturbed every 3 days, corresponding to a value of $N = 120/\text{yr}$. It will be shown that the contribution of the area where daily activity occurs is negligible so that it does not need to be treated separately in the calculations.



* A portion of C₂ is disturbed daily by reclaiming activities.

Area ID	$\frac{u_s}{u_r}$	Pile Surface	
		.%	Area (m ²)
A	0.9	12	101
B	0.6	48	402
C ₁ + C ₂	0.2	40	<u>335</u>
			838

Figure 3. Example 1: Pile surface areas within each wind speed regime.

Step 3: The calculation procedure involves determination of the fastest mile for each period of disturbance. Figure 4 shows a representative set of values (for a 1-month period) that are assumed to be applicable to the geographic area of the pile location. The values have been separated into 3-day periods, and the highest value in each period is indicated. In this example, the anemometer height is 7 m, so that a height correction to 10 m is needed for the fastest mile values. From Equation 10,

$$u_{10}^+ = u_7^+ \frac{\ln(10/0.005)}{\ln(7/0.005)}$$

$$u_{10}^+ = 1.05 u_7^+$$

Step 4: The next step is to convert the fastest mile value for each 3-day period into the equivalent friction velocities for each surface wind regime (i.e., u_s/u_r ratio) of the pile, using Equations 11 and 12. Figure 3 shows the surface wind speed pattern (expressed as a fraction of the approach wind speed at a height of 10 m). The surface areas lying within each wind speed regime are tabulated below the figure.

The calculated friction velocities are presented in Table 9. As indicated, only three of the periods contain a friction velocity which exceeds the threshold value of 1.12 m/s for an uncrusted coal pile. These three values all occur within the $u_s/u_r = 0.9$ regime of the pile surface.

TABLE 9. EXAMPLE 1: CALCULATION OF FRICTION VELOCITIES

3-Day period	u_7^+		u_{10}^+		u_s/u_r {	$u^* = 0.1 u_s^+$ (m/s)		
	(mph)	(m/s)	(mph)	(m/s)		0.2	0.6	0.9
1	14	6.3	15	6.6		0.13	0.40	0.59
2	29	13.0	31	13.7		0.27	0.82	1.23
3	30	13.4	32	14.1		0.28	0.84	1.27
4	31	13.9	33	14.6		0.29	0.88	1.31
5	22	9.8	23	10.3		0.21	0.62	0.93
6	21	9.4	22	9.9		0.20	0.59	0.89
7	16	7.2	17	7.6		0.15	0.46	0.68
8	25	11.2	26	11.8		0.24	0.71	1.06
9	17	7.6	18	8.0		0.16	0.48	0.72
10	13	5.8	14	6.1		0.12	0.37	0.55

Local Climatological Data

MONTHLY SUMMARY



WIND					DATE
RESULTANT DIR.	RESULTANT SPEED M.P.H.	AVERAGE SPEED M.P.H.	FASTEST MILE		
			SPEED M.P.H.	DIRECTION	
13	14	15	16	17	22
30	5.3	6.9	9	36	1
01	10.5	10.6	14	01	2
10	2.4	6.0	10	02	3
13	11.0	11.4	16	13	4
12	11.3	11.9	15	11	5
20	11.1	19.0	23	30	6
29	19.6	19.8	30	30	7
29	10.9	11.2	17	30	8
22	3.0	8.1	15	13	9
14	14.6	15.1	23	12	10
29	22.3	23.3	31	29	11
17	7.9	13.5	23	17	12
21	7.7	15.5	18	18	13
10	4.5	9.6	22	13	14
10	6.7	8.8	13	11	15
01	13.7	13.8	21	36	16
33	11.2	11.5	15	34	17
27	4.3	5.8	12	31	18
32	9.3	10.2	14	35	19
24	7.5	7.8	18	24	20
22	10.3	10.6	16	20	21
32	17.1	17.3	25	32	22
29	2.4	8.5	14	13	23
07	5.9	8.8	15	02	24
34	11.3	11.7	17	32	25
31	12.1	12.2	16	32	26
30	8.3	8.5	16	26	27
30	8.2	8.3	13	32	28
33	5.0	6.6	10	32	29
34	3.1	5.2	9	31	30
29	4.9	5.5	8	25	31
FOR THE MONTH:					
30	3.3	11.1	31	29	
					DATE: 11

Figure 4. Daily fastest miles of wind for periods of interest.

Step 5: This step is not necessary because there is only one frequency of disturbance used in the calculations. It is clear that the small area of daily disturbance (which lies entirely within the $u_s/u_r = 0.2$ regime) is never subject to wind speeds exceeding the threshold value.

Steps 6 and 7: The final set of calculations (shown in Table 10) involves the tabulation and summation of emissions for each disturbance period and for the affected subarea. The erosion potential (P) is calculated from Equation 8.

TABLE 10. EXAMPLE 1: CALCULATION OF PM-10 EMISSIONS^a

3-Day period	u^* (m/s)	$u^* - u_{\xi}^*$ (m/s)	P (g/m ²)	ID	Pile Surface		
					Area (m ²)	kPA (g)	
2	1.23	0.11	3.45	A	101	170	
3	1.27	0.15	5.06	A	101	260	
4	1.31	0.19	6.84	A	101	350	
Total PM ₁₀ emissions = 780							

^a where $u_{\xi}^* = 1.12$ m/s for uncrusted coal and $k = 0.5$ for PM-10.

For example, the calculation for the second 3-day period is:

$$P_2 = 58(1.23 - 1.12)^2 + 25(1.23 - 1.12) \\ = 0.70 + 2.75 = 3.45 \text{ g/m}^2$$

The PM-10 emissions generated by each event are found as the product of the PM-10 multiplier ($k = 0.5$), the erosion potential (P), and the affected area of the pile (A).

As shown in Table 10, the results of these calculations indicate a monthly PM-10 emission total of 780 g.

3.4 EXAMPLE CALCULATION--WIND EROSION FROM FLAT AREA COVERED WITH COAL DUST

A flat circular area of 29.2 m in diameter is covered with coal dust left over from the total reclaiming of a conical coal pile described in the example above. The total exposed surface area is calculated as follows:

$$S = \frac{\pi}{4} d^2 = 0.785 (29.2)^2 = 670 \text{ m}^2$$

This area will remain exposed for a period of 1 month when a new pile will be formed.

Step 1: In the absence of field data for estimating the threshold friction velocity, a value of 0.54 m/s is obtained from Table 7.

Step 2: The entire surface area is exposed for a period of 1 month after removal of a pile and $N = 1/\text{yr}$.

Step 3: From Figure 4, the highest value of fastest mile for the 30-day period (31 mph) occurs on the 11th day of the period. In this example, the reference anemometer height is 7 m so that a height correction is needed for the fastest mile value. From Step 3 of the previous example, $u_{10}^+ = 1.05 u_7^+$, so that $u_{10}^+ = 33$ mph.

Step 4: Equation 9 is used to convert the fastest mile value of 33 mph (14.6 m/s) to an equivalent friction velocity of 0.77 m/s. This value exceeds the threshold friction velocity from Step 1 so that erosion does occur.

Step 5: This step is not necessary because there is only one frequency of disturbance for the entire source area.

Steps 6 and 7: The PM-10 emissions generated by the erosion event are calculated as the product of the PM-10 multiplier ($k = 0.5$), the erosion potential (P) and the source area (A). The erosion potential is calculated from Equation 8 as follows:

$$\begin{aligned} P &= 58(0.77 - 0.54)^2 + 25(0.77 - 0.54) \\ &= 3.07 + 5.75 \\ &= 8.82 \text{ g/m}^2 \end{aligned}$$

Thus the PM-10 emissions for the 1-month period are found to be:

$$\begin{aligned} E &= (0.5)(8.82 \text{ g/m}^2)(670 \text{ m}^2) \\ &= 3.0 \text{ kg} \end{aligned}$$

4.0 REFERENCES

1. P. W. Kalika, R. E. Kenson, and P. T. Bartlett, Development of Procedures for the Measurement of Fugitive Emissions, EPA-600/2-76-284, U.S. Environmental Protection Agency, Research Triangle Park, North Carolina, 1976.
2. T. R. Blackwood, R. A. Wachter, Source Assessment: Coal Storage Piles, EPA Contract No. 68-02-1874, U.S. Environmental Protection Agency, Cincinnati, Ohio, July 1977.
3. PEDCo Environmental, Survey of Fugitive Dust from Coal Mines, EPA-908/1-78-003, U.S. Environmental Protection Agency, Denver, Colorado, February 1978.
4. R. A. Bagnold, The Physics of Blown Sand and Desert Dunes, Methuen, London, England, 265 pp., 1941.
5. D. A. Gillette, "Tests With a Portable Wind Tunnel for Determining Wind Erosion Threshold Velocities," *Atmospheric Environment*, 12:2309 (1978).
6. C. Cowherd, Jr., "Emission Factors for Wind Erosion of Exposed Aggregates at Surface Coal Mines," presented at the 75th Annual Meeting of the Air Pollution Control Association, New Orleans, Louisiana, June 1982.
7. E. Simiu, M. J. Changery, J. J. Filliben, "Extreme Wind Speeds at 129 Stations in the Contiguous United States," National Bureau of Standards Science Series 118, Washington, D.C., March 1979.
8. Chepil, W. S., "Improved Rotary Sieve for Measuring State and Stability of Dry Soil Structure," *Soil Science Society of America Proceedings*, 16:113-117, 1952.
9. Gillette, D. A., et al., "Threshold Velocities for Input of Soil Particles Into the Air By Desert Soils," *Journal of Geophysical Research*, 85(C10):5621-5630.
10. Local Climatological Data, Monthly Summary, Available for each U.S. Weather Station from the National Climatic Center, Asheville, NC 28801.
11. Changery, M. J., "National Wind Data Index Final Report," National Climatic Center, Asheville, NC, HCO/T1041-01 UC-60, December 1978.
12. Stunder, B. J. B., and S. P. S. Arya, "Windbreak Effectiveness for Storage Pile Fugitive Dust Control: A Wind Tunnel Study," *Journal of the Air Pollution Control Association*, 38:135-143, 1988.

APPENDIX A

ESTIMATION OF THRESHOLD FRICTION VELOCITY

For uncrusted surfaces, the threshold friction velocity is best estimated from the dry aggregate structure of the soil. A simple hand sieving test of surface soil is highly desirable to determine the mode of the surface aggregate size distribution by inspection of relative sieve catch amounts, following the procedure specified in Figure A-1 and Table A-1. The threshold friction velocity for erosion can be determined from the mode of the aggregate size distribution, following a relationship derived by Gillette (1980) as shown in Figure A-2.

A more approximate basis for determining threshold friction velocity would be based on hand sieving with just one sieve, but otherwise follows the procedure specified in Figure A-1. Based on the relationship developed by Bisal and Ferguson (1970), if more than 60% of the soil passes a 1-mm sieve, the "unlimited reservoir" model will apply; if not, the "limited reservoir" model will apply. This relationship has been verified by Gillette (1980) on desert soils.

If the soil contains nonerodible elements which are too large to include in the sieving (i.e., greater than about 1 cm in diameter), the effect of these elements must be taken into account by increasing the threshold friction velocity. Marshall (1971) has employed wind tunnel studies to quantify the increase in the threshold velocity for differing kinds of nonerodible elements. His results are depicted in terms of a graph of the rate of corrected to uncorrected friction velocity versus L_c (Figure A-3), where L_c is the ratio of the silhouette area of the roughness elements to the total area of the bare loose soil. The silhouette area of a nonerodible element is the projected frontal area normal to the wind direction.

A value for L_c is obtained by marking off a 1 m x 1 m surface area and determining the fraction of area, as viewed from directly overhead, that is occupied by nonerodible elements. Then the overhead area should be corrected to the equivalent frontal area; for example, if a spherical nonerodible element is half imbedded in the surface, the frontal area is one-half of the overhead area. Although it is difficult to estimate L_c for values below 0.05, the correction to friction velocity becomes less sensitive to the estimated value of L_c .

The difficulty in estimating L_c also increases for small nonerodible elements. However, because small nonerodible elements are more likely to be evenly distributed over the surface, it is usually acceptable to examine a smaller surface area, e.g., 30 cm x 30 cm.

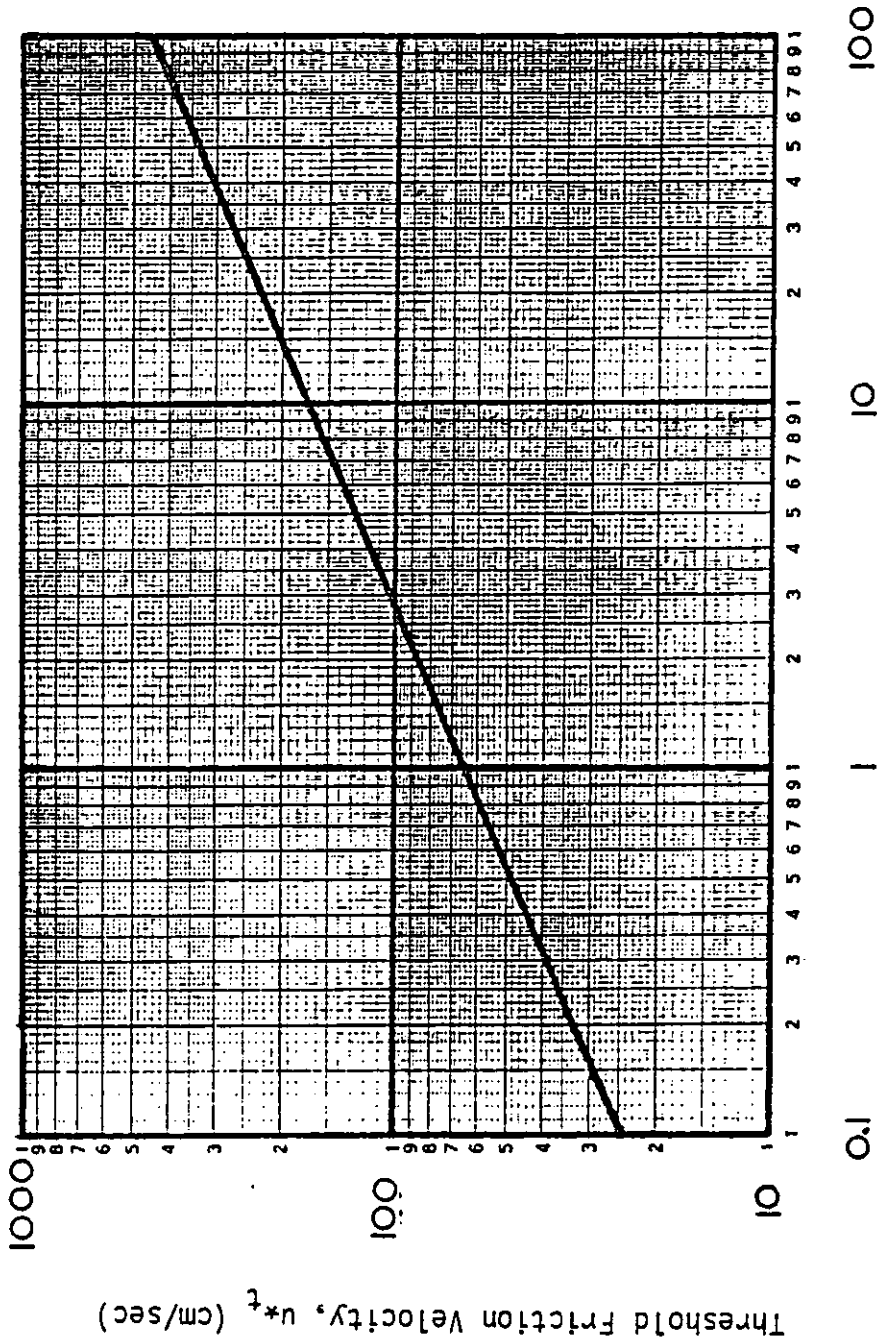
1. Prepare a nest of sieves with the following openings: 4 mm, 2 mm, 1 mm, 0.5 mm, 0.25 mm. Place a collector pan below the bottom sieve (0.25 mm opening).
2. Collect a sample representing the surface layer of loose particles (approximately 1 cm in depth for an encrusted surface), removing any rocks larger than about 1 cm in average physical diameter. The area to be sampled should not be less than 30 cm x 30 cm.
3. Pour the sample into the top sieve (4 mm opening), and place a lid on the top.
4. Rotate the covered sieve/pan unit by hand using broad sweeping arm motions in the horizontal plane. Complete 20 rotations at a speed just necessary to achieve some relative horizontal motion between the sieve and the particles.
5. Inspect the relative quantities of catch within each sieve and determine where the mode in the aggregate size distribution lies, i.e., between the opening size of the sieve with the largest catch and the opening size of the next largest sieve.
6. Determine the threshold friction velocity from Figure A-2 or Table A-1.

Figure A-1. Field procedure for determination of threshold friction velocity.*

* Adapted from a laboratory procedure published by W. S. Chepil (1952).

TABLE A-1. FIELD PROCEDURE FOR DETERMINATION OF
THRESHOLD FRICTION VELOCITY

Tyler sieve no.	Opening (mm)	Midpoint (mm)	u_t^* (cm/sec)
5	4		
		3	100
9	2		
		1.5	72
16	1		
		0.75	58
32	0.5		
		0.375	43
60	0.25		



Aggregate Size Distribution Mode (mm).

Figure A-2. Relationship of threshold friction velocity to size distribution mode.

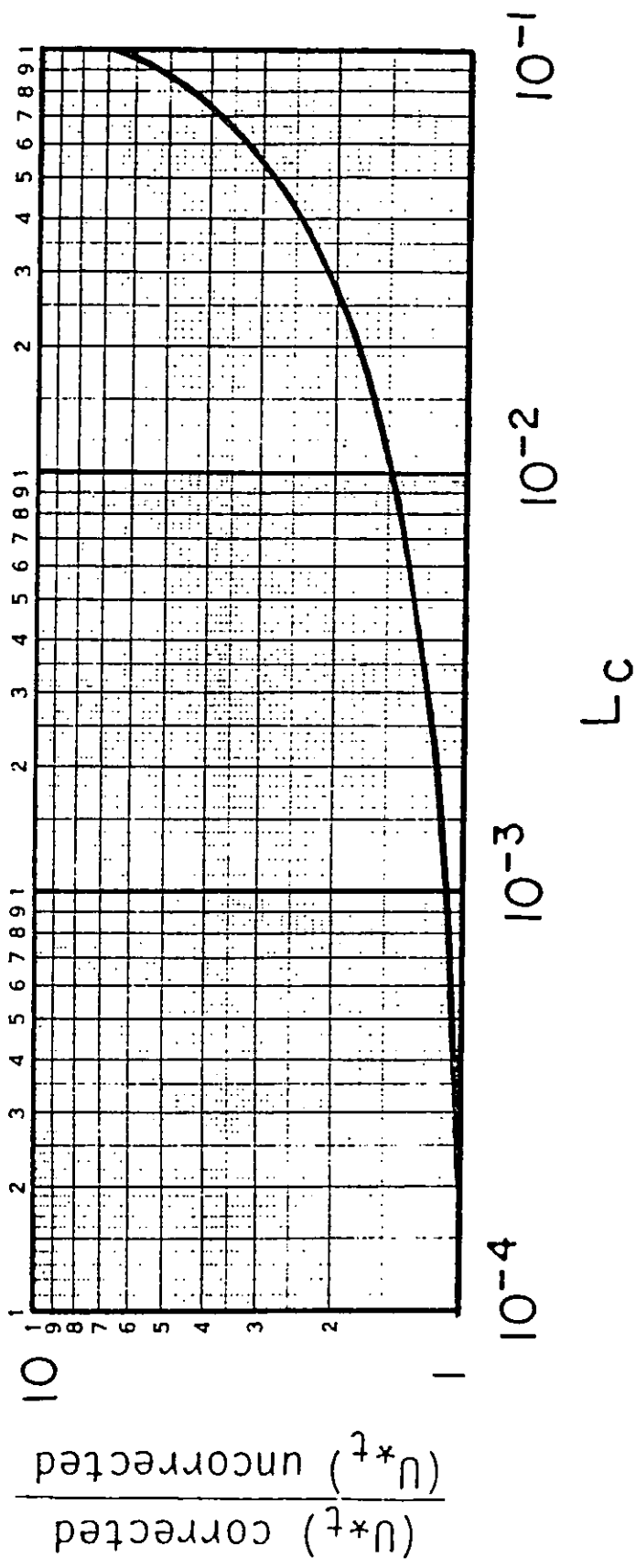


Figure A-3. Increase in threshold friction velocity with L_c .

REFERENCES FOR APPENDIX

- Bisal, F., and W. Ferguson. 1970. Effect of Nonerodible Aggregates and Wheat Stubble on Initiation of Soil Drifting. *Canadian Journal of Soil Science*, 50:31-34.
- Chepil, W. S. 1952. Improved Rotary Sieve for Measuring State and Stability of Dry Soil Structure. *Soil Science Society of American Proceedings*, 16:113-117.
- Gillette, D. A., et al. 1980. Threshold Velocities for Input of Soil Particles Into the Air by Desert Soils. *Journal of Geophysical Research*, 85(C10):5621-5630.
- Marshall, J. 1971. Drag Measurements in Roughness Arrays of Varying Density and Distribution. *Agricultural Meteorology*, 8:269-292.